A Three-Parameter Inferior Mirage Model for Optical Sensing of Surface Layer Temperature Profiles

WALDEMAR H. LEHN, SENIOR MEMBER, IEEE, AND JOHN S. MORRISH

Abstract—**Inferior mirages provide a sensitive and fairly accurate probe for determining vertical temperature distributions in the atmospheric surface layer. Optical measurements on the image can be used to calculate the parameters in a temperature profile model, in this case a function with three adjustable parameters. The function contains an exponential term (two parameters) and an additive linear term (one parameter). The optical observations, for which a known target is required, consist of the elevation angles of the apparent peak, caustic, and horizon. Analytic expressions that must be simultaneously satisfied are derived for all three conditions. The parameter values are extracted numerically by minimizing a positive definite function of the three conditions. The model is tested on a set of images for which nearly simultaneous photographs, theodolite readings, and temperature profiles were available. For each image the three calculated elevations matched the measured values very closely. The complete images also match well in most of the cases. The results, a distinct improvement over previous two-parameter models, also provide a more accurate reconstruction than is obtained from the thermodynamic model for unstable stratification.**

I. Introduction

OVER WATER or flat terrain, the vertical temperature profile of the atmospheric surface layer can be deduced by optical means. Measurements on the refraction of nearly horizontal light rays may be mathematically inverted to give a spatially averaged temperature structure along the line of sight. An early example of this approach is Fleagle's study of a layer, only a few meters thick, over water [1]. Sparkman [2], who concentrates on a two-parameter logarithmic profile at the surface, gives a large list of references to previous work in refraction.

An attractive two-parameter model for the inferior mirage is proposed by Fraser [3]. He develops a quadratic approximation to the thermodynamic equations that conventionally describe unstable stratification at the surface and finds a very convenient closed-form solution. His optical input data consist of two elevation measurements on a mirage image: the horizon and the caustic. The latter is the envelope of the rays, below which nothing can be seen by the observer. Its elevation on the target object is easily identified, for it appears as a line of "reflection" that divides the upper erect image from the inverted image below it.

Fraser's method takes no account of object information available above the caustic and for this reason experiences difficulties in predicting image behavior in this region. The field observations described below are the motivation for the present work, for they do not fit the Fraser model. The horizontal range of the observations is 20 km, over which distance the caustic elevation becomes much higher than eye level. At such elevations, Fraser's quadratic approximation for a steep lapse rate begins to turn into a temperature increase, i.e., the approximation is not valid over the elevation range encountered in this experiment.

In the following sections, a three-parameter model is developed to extend the horizontal and vertical range of the previous model [4]. It is evaluated in terms of field data by comparing computed with measured temperature profiles, and by comparing computed with photographed images. A comparison with the standard thermodynamic model is also made, showing that departures from it are necessary to predict the observed images.

II. The Three-Parameter Model

Various functional forms have been proposed to approximate the temperature profile of the surface layer. Temperature proportional to elevation plus square root of elevation (linear plus square root) is discussed in Pernter and Exner [5], based on experimental data. Theoretical analysis of the unstably stratified surface layer yields a logarithmic plus linear profile [6], also mentioned by Sparkman and used by Fraser [3] to derive his two parameter quadratic. Sparkman [2] also suggests a power law, but concentrates his attention on the logarithmic profile. An exponential variation of refractive index with elevation was proposed by Sodha *et al.* [7], which in an approximation for small total temperature variation implies an exponential plus linear law. This is the form chosen for the present analysis:

$$T - T_0 = \alpha(e^{-\beta z} - 1) - \gamma z \qquad (1)$$

where T is the temperature at elevation z, T_0 the temperature at $z = 0$ (sea level), and α, β, and γ are adjustable parameters. This function is simple, and possesses the necessary properties for appearance of a caustic, namely, maximum temperature gradient at the ground [3]. The parameter γ allows adjustment of the lapse rate at higher

Manuscript received February 18, 1986. This work was supported by the Natural Sciences and Engineering Research Council, Canada; the Department of Indian and Northern Affairs, Canada; the Polar Continental Shelf Project, Canada; and the Alexander von Humboldt Foundation, Federal Republic of Germany.

The authors are with the Department of Electrical Engineering, University of Manitoba, Winnipeg, Canada R3T 2N2.

IEEE Log Number 8610366.

elevations, necessary for matching measured peak elevations of known targets.

The optical field measurements needed to calculate the parameters are the apparent angular elevations of horizon, caustic, and peak of a known target. These points are obvious in a photograph or through a theodolite, and hence easy to measure. A theodolite reading to arc-seconds is recommended.

Three conditions that permit calculation of the parameters are conveniently derived using Fraser's transformed coordinates; the reader is referred to [3] for details, of which only a very brief summary appears here. The coordinates ξ_t, ζ_t of a point on a light ray are expressed in parametric form as two integrals

$$\xi_t = -2 \int_{\phi_e}^{\phi_t} \zeta' \, d\phi \tag{2}$$

$$\zeta_t = -2 \int_{\phi_e}^{\phi_t} \zeta' \phi \, d\phi \tag{3}$$

and

$$\zeta' \triangleq \frac{d\zeta}{d\tau} \tag{4}$$

where (approximately)

- ϕ is the local slope angle of the ray, relative to a circle concentric with the earth;
- ξ is the "horizontal" distance from the observer, measured along the earth's curvature;
- ζ is the elevation above the observer's eye level;
- τ is proportional to departure from eye level temperature;

and e, t are subscripts identifying eye and target values, respectively. With these variables, Snell's law assumes the form

$$\tau = \phi_e^2 - \phi^2. \tag{5}$$

Specifying a relation between τ and ζ (i.e., a temperature profile) permits the integrals to be evaluated, and ray paths to be found.

Specifically, the equation for τ is

$$\tau = A^{-1}[(T - T_e) - B\zeta] \tag{6}$$

where

- $A = \bar{T}^2/(1.58 \times 10^{-4}\,\bar{p})$
- $B = 2A/r_E - \gamma_a$
- T is the temperature in degrees, Kelvin
- p is the atmospheric pressure in millibars (typically 1013 mbar)
- r_E is the radius of the earth (6.37×10^6 m)
- $\gamma_a = 0.0342$°C/m

and the superscript bar denotes mean values for the observation under consideration.

In the transformed coordinates, the exponential plus linear profile appears as follows:

$$\tau = a(e^{-b\zeta} - 1) - c\zeta. \tag{7}$$

The three conditions required to compute the parameters a, b, and c are derived from this form, and (6) is used to find temperature T.

The horizon condition is the easiest to find: the horizon ray is tangential to the earth, at which point $\phi_t = 0$. The position of the ground relative to the observer's eye is ζ_s (a negative number), and (2) becomes

$$\zeta_s = -2 \int_{\phi_h}^{0} \zeta' \phi \, d\phi. \tag{8}$$

Here, ϕ_e has been renamed ϕ_h to identify the measured elevation angle of the horizon.

The peak condition requires iterative calculation because the value of ϕ_t is not known. For any selected temperature profile, ζ' is known. The apparent peak elevation (ϕ_e) and the target distance (ξ_t) are known from measurements. Hence the value of ϕ_t necessary to satisfy (2) may be found. This value when used in (3) gives the ray elevation at the target peak. The peak condition is thus a rewriting of (2), (3) with subscript p representing peak values

$$\xi_p = -2 \int_{\phi_p}^{\phi_t} \zeta' \, d\phi \tag{9}$$

$$\zeta_p = -2 \int_{\phi_p}^{\phi_t} \zeta' \phi \, d\phi. \tag{10}$$

The caustic condition is derived from two derivatives [3]: $d\xi_t/d\phi_e = 0$ and $d\zeta_t/d\phi_e = 0$. The second of these states that ζ_t is stationary with respect to ϕ_e on the caustic, and thus, from (7), τ_t is likewise stationary. From (5)

$$\tau_t = \phi_e^2 - \phi_t^2 \tag{11}$$

which, when the derivative with respect to ϕ_e is set to zero, yields

$$\frac{d\phi_t}{d\phi_e} = \frac{\phi_e}{\phi_t} \tag{12}$$

as obtained in [3].

The ξ derivative is found directly from (9)

$$0 = \frac{d\xi_t}{d\phi_e} = \int_{\phi_e}^{\phi_t} \frac{d\zeta'}{d\phi_e} d\phi + \zeta'(\phi_t) \frac{d\phi_t}{d\phi_e} - \zeta'(\phi_e). \tag{13}$$

The integrand is expressed as

$$\frac{d\zeta'}{d\phi_e} = \frac{d\zeta'}{d\zeta} \frac{d\zeta}{d\tau} \frac{d\tau}{d\phi_e} \tag{14}$$

and evaluated using (7) and (5). The result (12) is also substituted into (13) to produce, finally, the caustic condition

$$0 = \zeta'(\phi_t) \frac{\phi_c}{\phi_t} + \frac{1}{ab + c} + \int_{\phi_c}^{\phi_t} \frac{2ab^2 e^{-b\zeta} \phi_c}{(abe^{-b\zeta} + c)^3} d\phi \tag{15}$$

where ϕ_e has been rewritten as ϕ_c, to indicate the elevation angle of the caustic, as measured at the observer's position. The value of ϕ_t is found by the same iterative process as used with the peak condition, i.e., in (9), ϕ_p is replaced by ϕ_c.

Because an analytic closed-form solution is not available, an iterative strategy is required. Each of the three conditions (8), (10), and (15) is written as an expression equated to zero. The correct choice of the parameters of the temperature profile (a, b, c) will satisfy these conditions, whereas an incorrect choice will produce nonzero residuals. If the three residuals are appropriately combined into a single positive definite function, then minimization of this function with respect to a, b, and c will provide the best fit to the observations. The function selected is

$$I = 10^3|F_1| + 4|F_2| + |F_3| \tag{16}$$

where F_1, F_2, and F_3 are, respectively, the residuals from the caustic condition (15), the horizon condition (8), and the peak condition (10). The choice of weighting factors is discussed in the Appendix.

Ideally the correct parameters should give $I = 0$; in practice, the minimum values attained were not quite zero.

III. Experimental Results I

All of the field observations were carried out at Tuktoyaktuk, situated on the shores of the Beaufort Sea in the Canadian Arctic. Whitefish Summit, a low rounded hill easily identified on the horizon (Fig. 1), was selected as the optical target. Its distance from the observation point was 20 km. The height of its peak above sea level, measured on a local site survey, was 20.3 m. A 12-m mast supporting 12 thermistors at about 1-m intervals was erected on the sea ice 282 m from the observation point. The elevations of the camera and theodolite were 5.7 m above the ice. The map in Fig. 2 shows the significant points for this experiment.

Observations were taken over a 4-week period in May 1983. Five sets were identified for which nearly simultaneous photographs, theodolite measurements, and temperature readings were available; these sets were subjected to detailed analysis. Fig. 3 shows a typical case: the corners on the piecewise straight graph are thermistor readings, made on a digital meter to a precision of ± 0.1°C. Ray tracing based on such noisy data was considered pointless; rather, least squares curve fitting of quadratic and cubic functions was attempted. For each fit, rays were traced using previously reported methods [8], [9], and the corresponding image of Whitefish Summit was computed (Fig. 4). Neither computer image is even close to the observed image.

The difficulties were typical of all attempts to compute images on the basis of mast readings. As will be seen below, the noise level of ± 0.1°C is sufficient to prevent satisfactory image prediction.

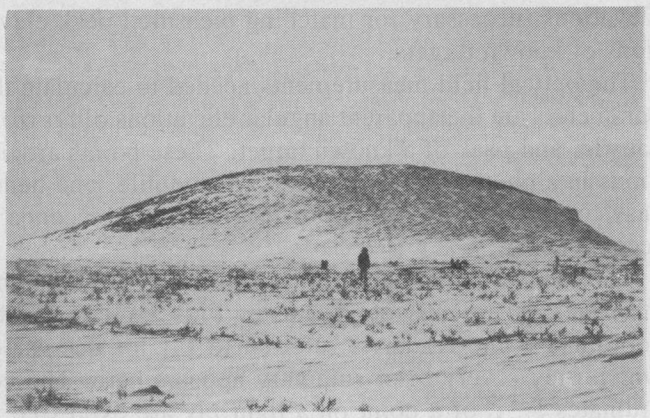

Fig. 1. Whitefish Summit, the target upon which the optical observations were made. The elevation of the center, beneath the small vertical post, is 20.3 m above sea level.

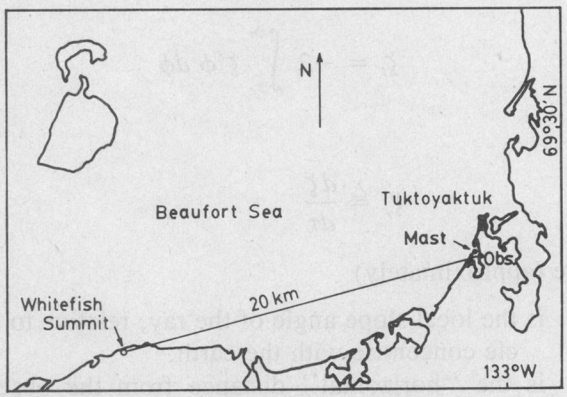

Fig. 2. Location plan.

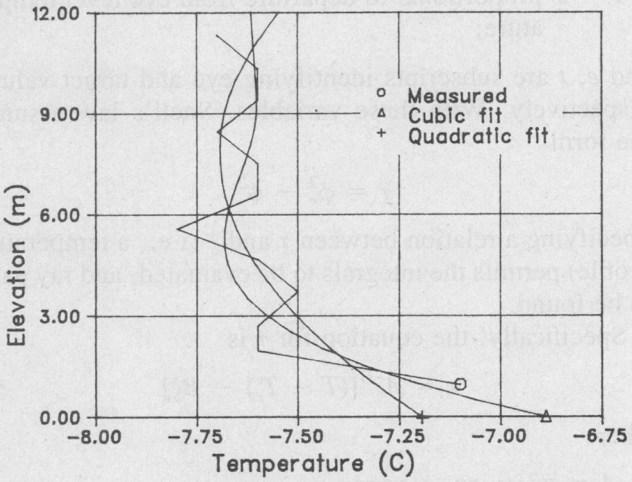

Fig. 3. A measured temperature profile with least squares fits. The measurements, made at 1946 h MDT on May 15, 1983, were the nearest in time to the theodolite readings of 1959 h. The quadratic fit was extended up to 20.3 m to compute the corresponding image. The cubic fit, however, was modified above 9.5 m to revert to the standard lapse rate of 0.006°/m.

IV. Experimental Results II

The three-parameter model, with values chosen to minimize (16), produces computed images that match the observations very well. Temperature readings from the mast

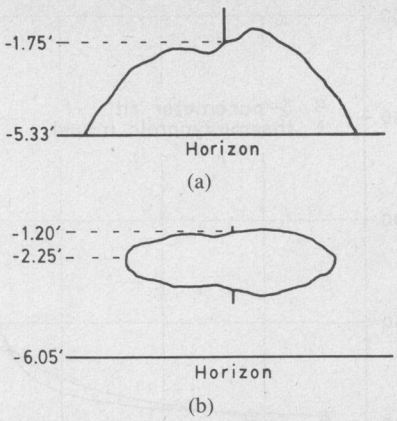

Fig. 4. (a) Image of Whitefish Summit that would be seen at the observation point for the quadratic fit to the temperature profile. (b) Computed image for the cubic fit profile. The actual image existing at the time is shown in Fig. 5.

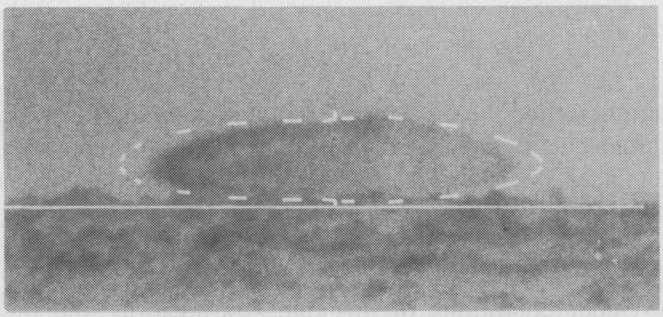

Fig. 5. Photograph of Whitefish Summit over the 20-km range from the observation point, made at 1955 h on May 15, 1983. The dotted lines show the computed image, based on the three parameter values that minimize (16) for the theodolite readings of 1959 h.

were used only to establish the eye level temperature (at elevation 5.7 m).

Fig. 5 shows the results calculated from theodolite readings made on May 15, 1983, at 1959 h Mountain Daylight Time (MDT). The photograph was made at 1955 h, and the mast was read at 1946 h. The minimum of (16) yielded the temperature profile (in degrees Celsius)

$$T = 0.26\, e^{-1.33z} - 0.0218z - 7.48. \qquad (17)$$

See the Appendix for an outline of the computation strategy. The profile (17) is shown in Fig. 6, superimposed on the mast readings; for most points it lies within the noise level of ± 0.1°C. Comparison of Figs. 3 and 6 and of the corresponding images shows how sensitive the image is to small changes in the profile. It becomes obvious that temperature profiling with ± 0.1°C measurements is simply not adequate to predict appropriate image shapes.

Figs. 7 to 10 show the three-parameter images for the remaining four cases selected. Table I compares the theodolite measurements with values computed by ray tracing for parameters minimizing (16). As expected, the errors are small. However, two of the images show departures from the calculated images. In Fig. 8, the photographed caustic is at an elevation different from the theodolite measurement. The time discrepancy was only 6 min between photograph and readings; based on observed rates

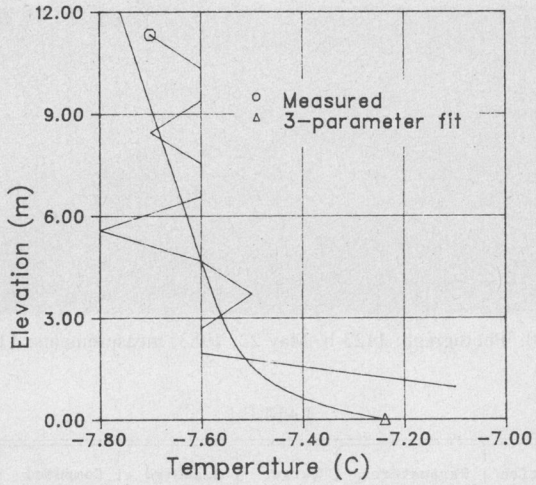

Fig. 6. The best three parameter fit for 1959 h, May 15, 1983, superimposed on the measurements of 1946 h.

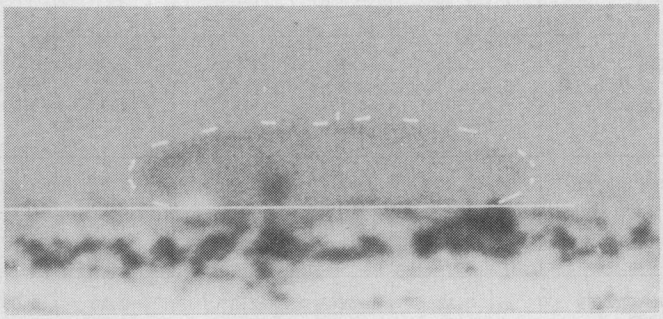

Fig. 7. Photograph of 1620 h, May 15, 1983, with image computed from the fit to the theodolite measurements of 1648 h.

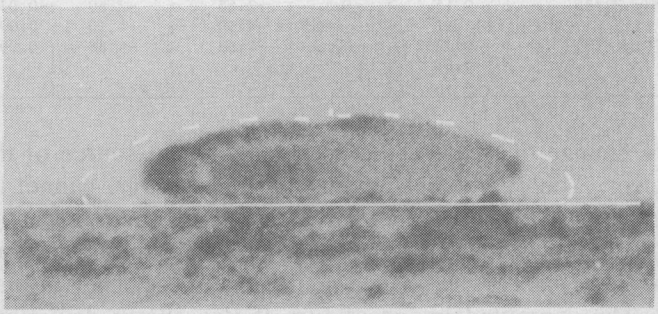

Fig. 8. Photograph: 1948 h, May 15, 1983; theodolite measurements: 1942 h. The computed image agrees with the measurements, which do not, however, agree with the photograph (see text).

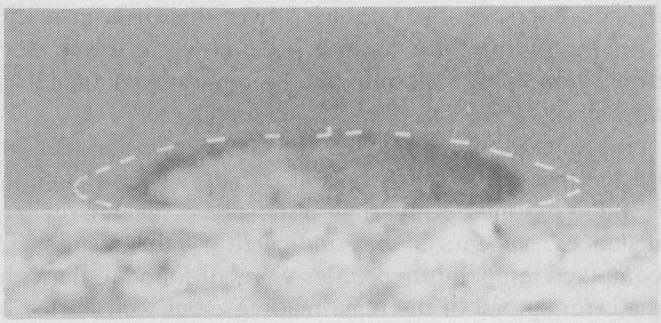

Fig. 9. Photograph: 1142 h, May 22, 1983; theodolite measurements: 1141 h. The elevations on the computed image agree with those of the photograph, but the computed image is too wide. This figure shows that the proposed three parameter fit is not always fully successful in describing the atmosphere along the observation range.

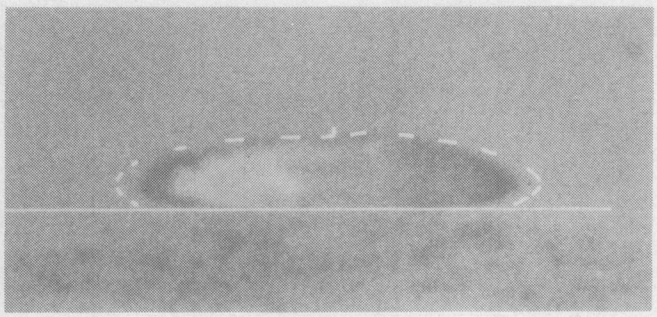

Fig. 10. Photograph: 1123 h, May 22, 1983; measurements: 1115 h.

TABLE I

Observation Time	Parameters for minimum I		Target	Measured Elevation	Computed Elevation	Error
May 15/83 1959 h (Fig. 5)	α	0.26	peak	-2.43	-2.41	-0.02
	β	1.33	caustic	-3.78	-3.78	0.00
	γ	0.0218	horizon	-4.85	-5.10	0.25
	δ	-7.48				
May 15/83 1648 h (Fig. 7)	α	0.24	peak	-2.33	-2.30	-0.03
	β	0.73	caustic	-3.92	-3.91	-0.01
	γ	0.0151	horizon	-4.95	-4.95	0.00
	δ	-6.32				
May 15/83 1942 h (Fig. 8)	α	0.17	peak	-1.88	-1.86	-0.02
	β	0.63	caustic	-4.07	-4.05	-0.02
	γ	0.00495	horizon	-4.58	-4.56	-0.02
	δ	-7.58				
May 22/83 1141 h (Fig. 9)	α	0.12	peak	-2.33	-2.30	-0.03
	β	1.88	caustic	-3.95	-3.94	-0.01
	γ	0.0198	horizon	-4.65	-4.69	0.04
	δ	-8.89				
May 22/83 1115 h (Fig. 10)	α	0.15	peak	-2.63	-2.60	-0.03
	β	1.02	caustic	-4.10	-4.10	0.00
	γ	0.0262	horizon	-4.88	-4.88	0.00
	δ	-8.85				

of change of images, this is not likely the source of the error. The occasional reading error, however, cannot be entirely ruled out. As seen in Table I, the relative spacing of the theodolite readings for Fig. 8 falls somewhat outside the pattern established by the rest of the observations.

The computed image of Fig. 9 also shows deviations from the photograph. In this case the elevations are consistent, but the computed image is too wide at the caustic. This occurs when the elevation at which the computed caustic intersects the target is lower than it is in reality, bringing more of the summit (i.e., down to lower elevations) into view. The present three-parameter model can do nothing to correct for such discrepancies.

In general, the proposed three-parameter model produces image fits of remarkable fidelity. The assumption of the horizontally invariant atmosphere, even over large distances, appears to be vindicated by the results. The computed temperature profiles were all found to lie within the error spread of the mast readings, but well buried beneath the noise.

A disadvantage of the three parameter model is the computational burden. Each evaluation of (16) requires the tracing of several rays, and many evaluations are required to find the minimum, even with a moderately good initial guess. For this reason it seems unprofitable to attempt an extension into four parameters (to reduce the error in Fig. 9).

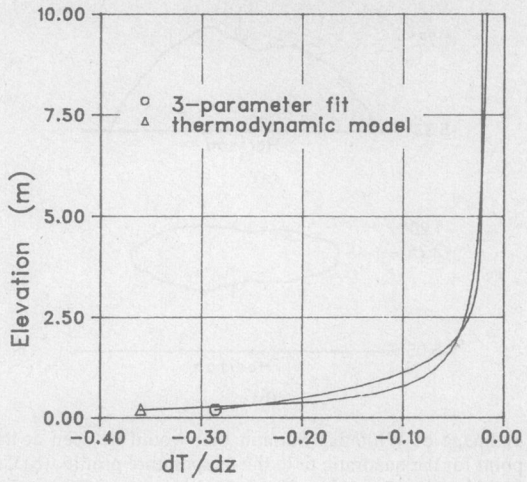

Fig. 11. Comparison of temperature gradients for the measurements of 1959 h, May 15, 1983. When the thermodynamic model was adjusted to approach the three parameter model as closely as possible (by visual estimate), the thermodynamic gradient took the form $dT/dz = -0.01 - 0.07/z$.

V. Comparison with the Thermodynamic Model

Under conditions of unstable stratification, the thermodynamic atmospheric model gives a temperature profile of the following form [6]:

$$T = \theta[\ln (z/z_0) - \Psi] - \Gamma z + T_0. \tag{18}$$

Comparison with the three-parameter model is most easily done using temperature gradients. Thus the gradient from (18) is

$$\frac{dT}{dz} = -\Gamma + \frac{\theta}{z} \tag{19}$$

where

$\Gamma = 0.01$, the adiabatic lapse rate;
$\theta = -(E_b/c_p \rho u_* k)$;
E_b is the buoyancy flux;
c_p is the specific heat of air at constant pressure;
ρ is the density of air;
k is the von Karman constant ($\simeq 0.4$);

and $u_* = kz\, \partial u/\partial z$, the friction velocity. Humidity effects can be ignored for the typical dry cold Arctic air.

The gradient for the three-parameter model is

$$\frac{dT}{dz} = -\alpha\beta\, e^{-\beta z} - \gamma \tag{20}$$

where α, β, and γ are related to the parameters a, b, and c by the scaling equations (see Appendix). Thus the gradient (20) is known, computed from measurements. The one parameter, θ, in the thermodynamic model (19) can now be adjusted to match (19) as closely as possible to (20); see graph in Fig. 11. The approximate heat flux from

TABLE II

Target	Measured Elevation	Computed Elevations		
		Three Parameter Model	Fraser Model	Thermodynamic Model
Peak	-2.43	-2.41	-1.27	-2.45
Caustic	-3.78	-3.78	-3.78	-4.10
Horizon	-4.85	-5.10	-4.84	-5.30

the surface could be estimated from θ and a wind speed measurement [10].

An image calculated by tracing rays through the best fit thermodynamic model does not fit the observations as well as the three-parameter model. Table II compares the computed values for the various models, for the theodolite observations of May 15, 1983, 1959 h. It is clear that departure from the thermodynamic model is necessary, if the observed images are to be reconstructed.

VI. Conclusions

A three-parameter model of exponential plus linear form has been developed for the temperature profiles that exist when the atmosphere is unstably stratified. This model reproduces observed inferior mirage images very accurately over horizontal ranges up to 20 km. Because it provides improved image representation, it must be considered an improvement in the estimation of the spatially averaged temperature profile between the observer and the target.

This study reinforces the idea that optical methods provide the simplest and most sensitive probes for determining micrometeorological temperature profiles.

Appendix

A. Scaling and Weighting Factors

In problems of terrestrial atmospheric refraction, there is always a wide disparity between the horizontal and vertical scales. Thus in the parametric ray equations (2) and (3), the orders of magnitude of the values are 10^4 m, 10 m, and 1 mrad, for ξ, ζ, and ϕ, respectively. Similarly, from (5), τ is an extremely small number. Scale factors were selected as follows, to bring the scaled numbers to sizes of the order of 10:

$$\tilde{\xi} = \xi/(3 \times 10^4) \tag{A1}$$

$$\tilde{\zeta} = \zeta \tag{A2}$$

$$\tilde{\phi} = 3 \times 10^4\, \phi \tag{A3}$$

$$\tilde{\tau} = 9 \times 10^8\, \tau \tag{A4}$$

Substitution of the scaled variables into the temperature profile (7) produces an equation of identical form, if scaled values for a, b, and c are defined as

$$\tilde{a} = 9 \times 10^8\, a \tag{A5}$$

$$\tilde{b} = b \tag{A6}$$

$$\tilde{c} = 9 \times 10^8\, c. \tag{A7}$$

TABLE III

Change in Measurement			Change in Residual		
$\Delta\tilde{\phi}_p$	$\Delta\tilde{\phi}_c$	$\Delta\tilde{\phi}_h$	Peak (F_3)	Caustic (F_1)	Horizon (F_2)
1	0	0	0.6	~0	~0
0	1	0	~0	0.0006	~0
0	0	1	~0	~0	0.15

The horizon, peak, and caustic conditions were evaluated in terms of scaled variables.

The weighting factors in (16) were selected to distribute angular errors equally between the three conditions, for cases where the minimum value was greater than zero. This distribution is consistent with the methods used in obtaining the three angle measurements by theodolite, i.e., the error in taking a reading was deemed likely to be the same for each of the three readings.

To find the weights, a point near the minimum was chosen for a typical case. Then each measurement, in turn, was incremented by a small amount, while the remaining measurements were held fixed, and the residuals of (8), (10), and (15) were calculated; see Table III.

Thus the residual F_3 was assigned unit weight, F_2 a weight of $0.6/0.15 = 4$, and F_1 by analogous calculation a weight of 1000. With these weights, and equal errors in the three angles, each term makes an equal contribution to I in (16).

B. Computational Strategy

The minimization of I requires adjustment of the parameters $\tilde{a}$, $\tilde{b}$, and $\tilde{c}$ in the scaled version of (7) for the profile $\tilde{\tau}$. This profile, after de-scaling, is inserted into (6) to convert temperature to ordinary degrees (Celsius or Kelvin)

$$T = T_e + A\tau + B\zeta. \tag{A8}$$

The reference elevation can be moved from eye level to sea level if ζ is replaced by $z + \zeta_s$. The result, temperature as a function of elevation above sea level, is

$$\begin{aligned} T &= T_e + Aa[e^{-b(z+\zeta_s)} - 1] - (Ac - B)(z + \zeta_s) \\ &= Aae^{-b\zeta_s} e^{-bz} - (Ac - B)z \\ &\quad + [T_e - Aa + (B - Ac)\zeta_s] \end{aligned} \tag{A9}$$

which may be rewritten as

$$T = \alpha e^{-\beta z} - \gamma z + \delta. \tag{A10}$$

This is the form originally proposed in (1), with $T_0 - \alpha$ replaced by δ.

Some experimentation with these functions showed that a direct search for a minimum of I by adjusting $\tilde{a}$, $\tilde{b}$, and $\tilde{c}$ was ill-conditioned. Changes in $\tilde{a}$ and $\tilde{b}$ tended to com-

pensate for each other, to produce very similar $T(z)$ functions, (A10), for significantly different $\tilde{a}$, $\tilde{b}$.

Minimization of (16) through variation of α, β, and γ in (A10) was more successful. Because refractive effects are dominated by temperature gradients, adjustments in the constant term δ have no significant effect on the image; hence, the value of δ was set at an estimated value and left fixed. The search through the remaining coordinates was executed as a kind of two-dimensional process: for a trial point α, β, the value of γ was adjusted to give minimum I. This somewhat tedious search through the α, β plane, with the subsidiary γ minimization at each point, was able to identify the minima of I with no difficulty.

References

[1] R. G. Fleagle, "The optical measurement of lapse rate," *Bull. Amer. Meteorol. Soc.*, vol. 31, pp. 51–55, 1950.

[2] J. K. Sparkman, "A remote sensing technique using terrestrial refraction, for the study of low-level lapse rate," Ph.D. dissertation, Univ. of Wisconsin, 1971.

[3] A. B. Fraser, "Simple solution for obtaining a temperature profile from the inferior mirage," *Appl. Opt.*, vol. 18, pp. 1724–1731, 1979.

[4] J. S. Morrish, "Inferior mirages and their corresponding temperature structures," M.Sc. thesis, Univ. of Manitoba, 1985.

[5] J. M. Pernter and F. M. Exner, *Meteorologische Optik*, 2nd ed. Vienna: Braumüller, 1922.

[6] R. G. Fleagle and J. A. Businger, *An Introduction to Atmospheric Physics*. New York: Academic, 1963.

[7] M. S. Sodha, A. K. Aggarwal, and P. K. Kaw, "Image formation by an optically stratified medium: optics of mirage and looming," *Brit. J. Appl. Phys.*, vol. 18, pp. 503–511, 1967.

[8] W. H. Lehn, "A simple parabolic model for the optics of the atmospheric surface layer," *Appl. Math. Modelling*, vol. 9, pp. 447–453, 1985.

[9] W. H. Lehn and H. L. Sawatzky, "Image transmission under arctic mirage conditions," *Polarforschung*, vol. 45, pp. 120–128, 1975.

[10] G. J. Haltiner and F. L. Martin, *Dynamical and Physical Meteorology*. New York: McGraw-Hill, 1957.

*

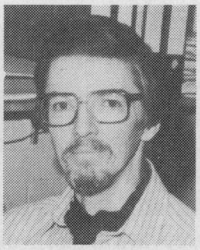

Waldemar H. Lehn (M'63–SM'81) received the B.Sc. degree in engineering physics from the University of Manitoba in 1961 and the M.Sc. (E.E.) degree from the Massachusetts Institute of Technology in 1962.

Since then he has been on the academic staff of the University of Manitoba, where he is presently Professor in the Department of Electrical Engineering. Two years of research leave have been spent in Germany: 1974–1975, as Visiting Professor at the University of Stuttgart, and 1981–1982, as Alexander von Humboldt Research Fellow at the University of Freiburg. His research interests center on optical propagation in the atmosphere and meteorological optics.

Mr. Lehn is a member of the Optical Society of America, Sigma Xi, and the Society of Photo-Optical Instrumentation Engineers, and he is a Registered Professional Engineer of the Province of Manitoba.

*

John S. Morrish received the B.Sc. (E.E.) degree in 1981 and the M.Sc. degree in 1985, both in electrical engineering from the University of Manitoba, Winnipeg, Manitoba.

He is currently in the Department of Geological Sciences at the University of Manitoba conducting research in remote sensing.